Temporal response and first order volume changes during grating formation in photopolymers

John V. Kelly, Michael R. Gleeson, Ciara E. Close, Feidhlim T. O'Neill, and John T. Sheridan[a)]
UCD School of Electrical, Electronic and Mechanical Engineering, University College Dublin, Belfield, Dublin 4, Ireland

Sergi Gallego and Cristian Neipp
Departamento de Física, Ingeniería de Sistemas y Teoría de la Señal, Universidad de Alicante, Apartado 99, E-03080 Alicante, Spain and Departamento Interuniversitario de Optica, Universidad de Alicante, Apartado 99, E-03080 Alicante, Spain

(Received 9 February 2006; accepted 28 March 2006; published online 6 June 2006)

We examine the evolution of the refractive index modulation when recording gratings in an acrylamide based photopolymer. A nonlocal diffusion model is used to predict theoretically the grating evolution. The model has been developed to account for both nonlocal spatial and temporal effects in the medium, which can be attributed to polymer chain growth. Previously it was assumed that the temporal effect of chain growth could be neglected. However, temporal effects due to chain growth and monomer diffusion are shown to be significant, particularly over short recording periods where dark field amplification is observed. The diffusion model is solved using a finite-difference technique to predict the evolution of the monomer and polymer concentrations throughout grating recording. Using independently measured refractive index values for each component of the recording medium, the Lorentz-Lorenz relation is used to determine the corresponding refractive index modulation. The corresponding diffraction efficiency is then determined using rigorous coupled wave analysis. The diffraction efficiency curves are presented for gratings recorded using short exposure times, monitored in real time, both during and after recording. The effect of volume shrinkage of polymer on grating evolution is also examined. Both the nonlocal temporal response of the material and monomer diffusion are shown to influence refractive index modulation postexposure. © *2006 American Institute of Physics*. [DOI: 10.1063/1.2200400]

I. INTRODUCTION

With current technologies reaching the limit of their storage capabilities the optical data industry is searching for the next generation of storage system to meet the demands of the digital age.[1] One possible solution is the use of holographic techniques where terabit capacity has been predicted and photopolymers are proving to be the recording medium of choice.[2]

It is necessary, however, to develop accurate models which describe the behavior of photopolymer. As noted, development of such models is critical for many applications including holographic data storage[3,4] and holographic optical element[5–7] fabrication and photoembossing.[8] Many such models have been proposed. Zhao and Mouroulis[9] proposed a model, which described the evolution of grating formation in photopolymer using a four harmonic expansion of the standard one-dimensional (1D) diffusion equation. Sheridan and Lawrence developed the nonlocal polymer driven diffusion model (NPDD) which extended the Zhao and Mouroulis model to include a nonlocal spatial response to account for high spatial frequency cutoff—Model I.[10] A square root relationship, shown to exist between the polymerization rate and the illuminating intensity,[11,12] was also incorporated—Model II.[13,14] Kinetics of the polymerization process has recently been examined[15,16] when the chain termination mechanism is either bimolecular (two chains terminating mutually) or primary (chain terminated with a free radical)—Model III.

In this paper we first extend Model II to account for volume changes occurring in the recording material during the recording process. Karpov *et al.*[17] and Sutherland *et al.*[18] have examined the effect of shrinkage in photopolymer. Both assume that free volume is created when monomer is converted to polymer. This is the due to the fact that the covalent single carbon bond in the polymer is up to 50% shorter than the van der Waals bond in the liquid monomer state. To model this, Sutherland *et al.* assumes that this results in the formation of temporary holes, which then collapse resulting in an overall reduction in the system volume. Karpov *et al.* allow for the diffusion of these holes throughout the medium. We assume hole collapse occurs quickly as the vacuum is filled and therefore, in this case, make the assumption that diffusion of holes is negligible. We then incorporate this behavior into the NPDD model.

The temporal response of the recording material is then examined and a material response function proposed. The model is solved using a finite-difference time-domain method [19] (FDTD) and the effects of the nonlocal temporal response on refractive index modulation using the Lorentz-

[a)]Author to whom correspondence should be addressed; FAX: +353-1-716-1927; electronic mail: john.sheridan@ucd.ie

Lorenz relation are examined.[20] These results are used to calculate diffraction efficiency using rigorous coupled wave analysis[21] (RCWA) and to carry out fits to experimental data.

An inhibition process has been noted at the beginning of the recording process. This can be attributed to deactivation of excited dye molecules due to the presence of oxygen in the material.[22] Models have recently been developed to describe this phenomenon.[23] In this paper, however, we neglect this dead band region when fitting our experimental data and assume that once this inhibition is overcome the recording process in unaffected by the presence of oxygen.

II. NONLOCAL POLYMERIZATION DRIVEN DIFFUSION (NPDD) MODEL

The generalized 1D NPDD partial differential equation describing photopolymerization in photopolymer can be written in the form

$$\frac{\partial u(x,t)}{\partial t} = \frac{\partial}{\partial x}\left[D(x,t)\frac{\partial u(x,t)}{\partial x}\right] - \int_{-\infty}^{+\infty}\int_{0}^{t} R(x,x';t,t') \times F(x',t')[u(x',t')]^{\beta} dt'\,dx' - \frac{u(x,t)}{u(x,t)+N(x,t)}\frac{\partial H(x,t)}{\partial t}, \tag{1}$$

where $u(x,t)$ is the free-monomer concentration, $D(x,t)$ is the monomer diffusion constant, $F(x,t)$ is the polymerization rate, $N(x,t)$ is the polymer concentration, $R(x,x';t,t')$ is the nonlocal response function,[10,13] $H(x,t)$ is the hole concentration, and β is a factor introduced to specify the dominant chain termination mechanism, either bimolecular ($\beta=1$) or primary ($\beta=2$).[15] In this paper we examine the bimolecular case, $\beta=1$.

A. Volume shrinkage

We assume that after a certain transience period the rate of hole creation will be approximately equal to the rate of hole collapse, and therefore we assume $\partial H(h,t)/\partial t$ is small and can be neglected from Eq. (1). This is a first order approximation and is valid as long as both the rate of hole formation occurring and the volume fraction of holes generated are low. The equation describing the hole formation system can be written as

$$\frac{\partial H(x,t)}{\partial t} = \rho\int_{-\infty}^{+\infty}\int_{0}^{t} R(x,x';t,t')F(x',t')[u(x',t')]^{\beta} dt'\,dx' - k_H H(x,t), \tag{2}$$

where ρ is the fraction of free volume created for each double bond conversion and k_H is the rate constant associated with hole collapse. Later in Sec. III, we present the numerical results describing the effect of shrinkage on polymer grating formation. The harmonics of hole composition can be determined where $H(x,t)=\Sigma_i H_i(t)\cos(iKx)$ and H_i is the ith harmonic component of hole concentration and $K=2\pi/\Lambda$, where Λ is the grating fringe spacing.

B. Nonlocal temporal response

The nonlocal response function represents the effect of monomer concentration at location x' and t' on the amount of material being polymerized at location x and time t. Radical chain polymerization results in chain growth away from the point of initiation. The active tip of each chain combines with free monomer extending the polymer chain. This results in polymerization occurring nonlocal to the point of initiation as a function of both time and space. Previously[10] we assumed that following a brief transient period, the spatial effect of chain growth was instantaneous (local in time or action at a distance). However, where the use of short exposures is necessary, as in optical data storage, temporal effects become more significant.

It is assumed that the nonlocal response function can be broken up into the product of a spatial and a temporal response, $R(x,x';t,t')=R(x,x')T(t,t')$. The purely temporal part of the response function takes account of the removal of monomer due to past initiations, over the time interval $0\leqslant t'<t$. In the local limit, the time response function must have the following mathematical properties:

$$\lim_{T_{\max}\to 0}\{T(t',t)\} = \delta(t'-t), \tag{3a}$$

$$\int_{-\infty}^{t} T(t',t)dt' = 1. \tag{3b}$$

Previously it was argued that only events in the recent past, quantified using $T_{\max}$, give rise to significant nonlocal temporal effects and that at any time after $T_{\max}$ any change in monomer concentration at x' will give rise to an instantaneous change in the amount of polymerization at x. The time response was therefore assumed to have the property that

$$\int_{t-T_{\max}}^{t} T(t',t)dt' \approx 1, \tag{4}$$

where $T_{\max}$ was defined as the maximum effective travel time between x and x'.[10] Under this assumption, the material response function reduces to a purely spatial response. This assumption is clearly questionable at times close to zero before the average number of chains reaching a point has reached a steady state and it can be assumed that only slow adiabatic variations to the steady state occur with respect to time. In this paper we no longer make this assumption but extend the nonlocal diffusion model to include both a nonlocal temporal and spatial response.

The effect of a chain initiated at time t' and position x' on the amount of polymer generated at time t and position x will decrease as the interval $t-t'$ increases. The biggest contribution to the removal of monomer at a point and time in space will be due to chains initiated at the same position and time. One possible temporal response function was determined to be the area normalized exponential function,

$$T(t-t') = \frac{1}{\tau_n}\exp\left[\frac{(t-t')}{\tau_n}\right], \tag{5}$$

where the time constant τ_n determines the extent of the nonlocal temporal response. As τ_n gets smaller the response be-

comes more localized and $T(t-t')$ approaches a delta function. The effects of introducing the nonlocal temporal response are discussed in the next section.

III. NUMERICAL SIMULATIONS

Previously the nonlocal model has been solved using a two or four harmonic expansion.[10,13] Recently it has been shown that for certain parameter values a more rigorous method for solving the nonlocal diffusion equation may be necessary. Wu and Glytsis[19] applied a FDTD method to solve the nonlocal diffusion equation (Model II) in its dimensionless form. Recently this method has been applied to solve the extended model, which includes the nonlocal temporal response.[24] It is important to consider sampling size when using this numerical method for both stability and accuracy. For numerical stability the increment in the time domain, Δt_D, must satisfy the stability criterion,[19]

$$\Delta t_D \leqslant \frac{1}{2}\frac{{\Delta x_D}^2}{R_D}, \tag{6a}$$

where R_D is a model parameter describing the relationship between the rate of polymerization and diffusion and Δx_D is the dimensionless time step. In most cases we choose $\Delta t_D = 0.4$ $({\Delta x_D}^2/R_D)$, which is consistent with the Wu and Glytsis analysis.[19] However, the diffusion model now includes a time integral. In evaluating this integral, using the trapezoidal rule, the size of Δt_D is critical to the numerical accuracy of the result. To estimate a suitable value of Δt_D, we examine the truncation error associated with the trapezoidal rule. Using the Taylor series it can be shown that the modulus of the truncation error, $|e|$, for the integral, $\int_0^{t_D'} T(t_D, t_D')dt_D$, is given by[25]

$$|e| \leqslant \frac{1}{12}{\Delta t_D}^2 |T''(\tau)| t_D, \tag{6b}$$

where $|T''(\tau)| = \max\{|T(x, t_D')|; 0 \leqslant x \leqslant t_D'\}$.

By choosing a suitable value for the maximum allowable truncation error in our system, we can then estimate an appropriate value for Δt_D. The truncation error used was $|e| = 0.005$.

The NPDD model is solved for the harmonic components of monomer, polymer, and hole concentration during grating formation. Previously, as discussed in Sec. II, it has been assumed that rates of polymerization respond instantaneously to changes in light intensity, i.e., there is no temporal response. Therefore if illumination is stopped during grating formation, polymerization stops instantaneously. Based on the above analysis and assuming that all the monomer has not been consumed completely by the end of illumination, we would expect initiated chains to continue growing after exposure before terminating some short time after. Colvin *et al.*[26] examined the harmonic evolution of polymer after exposure. However, any subsequent change in the harmonic amplitude was attributed solely to monomer diffusion and the effects of "dark reactions," i.e., continued polymer growth after illumination, were ignored. In this section we examine the effects of the inclusion of a nonlocal temporal response on harmonic evolution postexposure while considerable unpolymerized monomer still remains available in the material and we also examine the influence of polymer shrinkage.

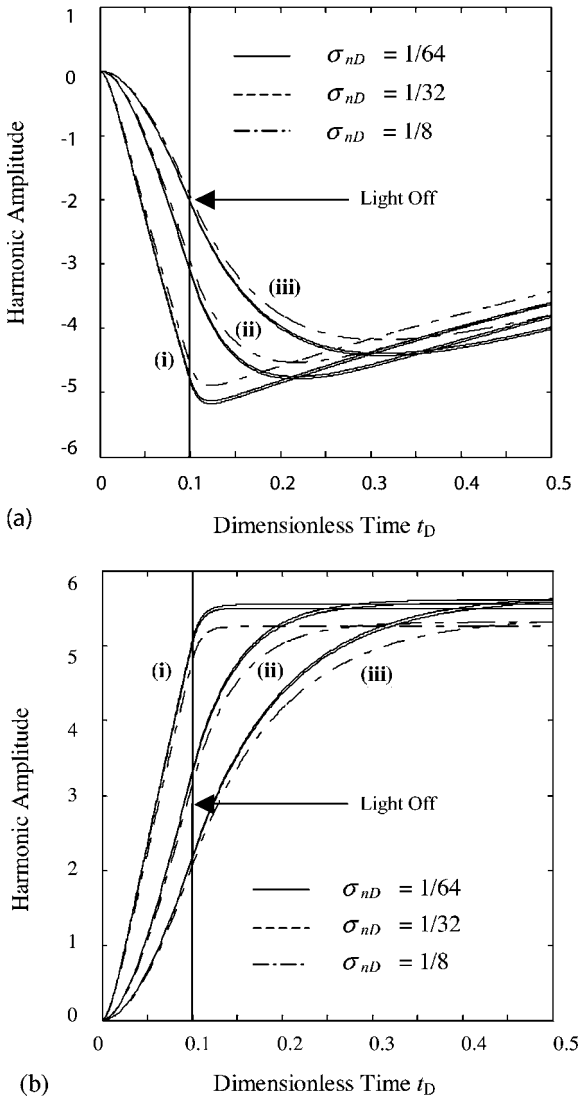

FIG. 1. First harmonic coefficient of (a) monomer concentration and (b) polymer concentration for values of $\sigma_{nD} = (1/64, 1/32, 1/8)$ and $\tau_{nD} =$ (i) 0.01, (ii) 0.05, and (iii) 0.1 where $R_D = 1$ and $\beta = 1$.

A. Effect of temporal response

Figure 1 shows the effect of dimensionless spatial and temporal nonlocal parameters, σ_{nD} and τ_{nD}, respectively, on the polymer and monomer first harmonic evolution when recording is stopped after t_D (dimensionless time) $= 0.1$ and where $\beta = 1$.

For small values of τ_{nD} we see that there is little increase in polymer harmonic amplitude after exposure has stopped. However, as the value of τ_{nD} increases the amplitude of the polymer harmonic continues to increase significantly before saturating. Similarly the monomer harmonic amplitude decreases as the monomer diffuses back into the depleted regions of the grating layer. Assuming chain termination is not

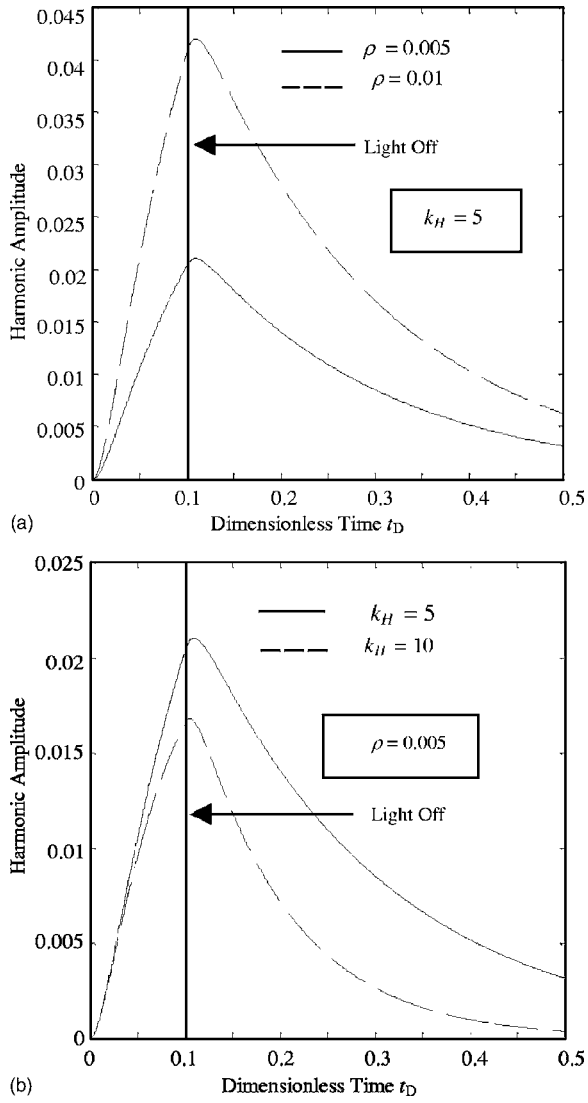

FIG. 2. Dependence of the first harmonic amplitude of hole concentration on (a) ρ, the fraction of free volume created during polymerization, and (b) the rate at which that free volume collapses, k_H. In each case $R_D=1$, $\beta=1$, $\sigma_D=0$, and $\tau_{nD}=0.01$.

instantaneous once exposure has stopped, and based on the above simulation, we see continued polymerization for a short period after exposure.

B. Effect of hole formation

The rate at which holes are generated and collapsed will depend on the characteristics of the material system being examined. Here we examine the effects of a number of different possible parameter values. Figure 2 shows the first harmonic of hole concentration, $H_1(x,t_D)$, for two different values of ρ.

Holes are generated as polymer is formed during the recording process. When recording stops we see the holes continue to collapse. For longer exposures the hole concentration will decrease before reaching a constant value, during the process. In this case, however, the rate of collapse never exceeds the rate of generation during the brief recording period and therefore never reaches a steady state value. However, as discussed in Sec. II, given the slow rate of hole generation and collapse, and the low concentration of holes generated in this period, our first order approximation appears valid. In the next section we examine the influence of hole formation on the refractive index modulation.

TABLE I. Concentrations and volume fractions of photopolymer material components.

Component	Mass (g)	Density (g/cm^3)	Volume (cm^3)	Volume fraction
PVA	7	1.3	5.384 615	0.333 025
Acrylamide	2.4	1.122	2.139 037	0.132 294
Bisacrylamide	0.8	1.24	0.645 161	0.039 902
TEA	8.992	1.124	8	0.494 78

IV. REFRACTIVE INDEX MODULATION EVOLUTION

In this section we present the measured values of the refractive index of the main components of the photopolymer recording material. We then examine the influence of these refractive index values on the first harmonic of refractive index modulation.

A. Refractive index measurements

The unpolymerized acrylamide based photopolymer holographic recording material used contains a monomer: acrylamide, a binder: polyvinylalcohol (PVA), a cross-linker: bisacrylamide, a dye: erythrosin B, and an electron donor: triethanolamine (TEA). The concentrations of each component are given in Table I.

A Metricon 2010 prism coupler[27] in thick film/bulk material index mode was used in our refractive index measurements. Solutions containing different combinations of material components were prepared and then allowed to dry on glass slides. The refractive indices of the layers were then measured at a wavelength of 633 nm. The results are given in Table II.

The refractive index of the material is dependent upon the refractive index of the individual material components and their concentrations or volume fractions. We assume that the material is made up mainly of monomer, polymer, and a background material (PVA+TEA). However, we also need to account for the influence of the free volume created due to hole formation during the recording process. Therefore assuming that volume is conserved[18,20] we can write

TABLE II. Refractive index measurements of material components (uncertainties based on repeated measurements).

Material	Refractive index
PVA	1.512 7
PVA+TEA	1.495 75±0.000 25
PVA+TEA+DYE	1.496 5±0.000 2
PVA+TEA+acrylamide	1.492 4
PVA+TEA+acrylamide+dye	1.494 1
PVA+TEA+acrylamide+bisacrylamide	1.494 8
PVA+TEA+acrylamide+bisacrylamide+dye	1.479 9±0.000 6

TABLE III. Refractive index values of material components found in the literature and those calculated from the results in Table II in conjunction with the Lorentz-Lorenz relation.

Chemical	Refractive index, $n^{\text{literature}}$	Refractive index, $n^{\text{calculated}}$
PVA	1.52–1.55[a]	1.512 7
TEA	1.485[b]	1.484 46
Acrylamide	$n_x=1.46$, $n_y=1.55$, $n_z=1.581$[c]	1.471 62

[a]Reference 28.
[b]Reference 29.
[c]Reference 30.

$$\phi^{(m)} + \phi^{(p)} + \phi^{(b)} + \phi^{(H)} = 1, \tag{7}$$

where $\phi^{(m)}$, $\phi^{(p)}$, $\phi^{(b)}$, and $\phi^{(H)}$ are the volume fractions monomer, polymer, background and holes respectively. While the collapse of holes will result in a reduction in the overall volume, the total volume fraction is by definition conserved. The total refractive index can then be expressed using the Lorentz-Lorenz relation,[20]

$$\frac{n^2-1}{n^2+2} = \phi^{(m)}\frac{{n_m}^2-1}{{n_m}^2+2} + \phi^{(p)}\frac{{n_p}^2-1}{{n_p}^2+2} + \phi^{(b)}\frac{{n_b}^2-1}{{n_b}^2+2} + \phi^{(H)}\frac{{n_H}^2-1}{{n_H}^2+2}, \tag{8}$$

where n_m, n_p, n_b, and n_H, are the refractive indices of monomer, polymer, background, and holes, respectively. We assume that the $n_H=1$, (i.e., *in vacuo*). The volume fraction is given by $\phi_i=x_i\nu_i/\Sigma_i x_i\nu_i$, where x_i is the mole fraction and ν_i is the molar volume of the ith component.

Using the data from Tables I and II and Eq. (8), the refractive index values for the main components of the material were estimated. The results are shown in the Table III. The calculated values of refractive index for PVA and TEA agree closely with those in the literature.[28,29] Independent verification of our measured value for the refractive index value of acrylamide is less clear as it is dependent on the form of the material.[30] However, having used the same method to extract the refractive index for the previous two components, we believe our result to be accurate. We note that the refractive index values are estimated for dry layers at 633 nm, which replicates grating experimental conditions.

The values presented in Table III are now used to examine the theoretical temporal evolution of refractive index modulation during the formation of transmission holographic gratings in the photopolymer described in Table I.

B. Refractive index modulation

Using Eq. (8) and following the analysis of Aubrecht *et al.*[20] and Kelly *et al.*,[24] the refractive index modulation can be written as

$$n_1 = \frac{({n_{\text{dark}}}^2+2)^2}{6n_{\text{dark}}}\left[\phi_1^{(m)}\left(\frac{{n_m}^2-1}{{n_m}^2+2}-\frac{{n_b}^2-1}{{n_b}^2+2}\right) + \phi_1^{(p)}\left(\frac{{n_p}^2-1}{{n_p}^2+2}-\frac{{n_b}^2-1}{{n_b}^2+2}\right) - \phi_1^{(H)}\left(\frac{{n_b}^2-1}{{n_b}^2+2}\right)\right], \tag{9}$$

where n_{dark} is the average refractive index of the material before exposure. $\phi_1^{(m)}$, $\phi_1^{(p)}$, and $\phi_1^{(H)}$ are the first harmonic components of monomer, polymer, and hole concentration, respectively. The refractive index values for monomer and binder are those shown in Table I. We can then estimate n_{dark} using Eq. (9) with the initial volume fraction of monomer, $\phi_1^{(m)}$, taken to be 0.13. This gives $n_{\text{dark}}\approx 1.49$. Using Eq. (9) and the harmonic values determined in Sec. III we now examine the evolution of the refractive index modulation as a function of time.

Figure 3 shows a plot of the first harmonic of refractive index modulation for different values of the hole generation factor ρ. As expected based on the NPDD model with nonlocal temporal response, we observe postexposure amplification as a result of dark field reactions. Now, however, we also take into account the effect of monomer diffusion after exposure. The values estimated for the refractive index of the monomer and background indicate $n_b > n_m$. Therefore, as the monomer diffuses back into the polymerized regions postexposure, the refractive index in these regions is reduced and hence the refractive index modulation decreases. The effect of hole generation and collapse can also be seen. The initial growth in refractive index modulation is reduced due to the presence of holes, having a refractive index value of $n_H=1$. Postexposure, however, two opposing processes exist. Collapsing holes will cause the refractive index modulation to increase while the diffusion of monomer will continue to cause a reduction in the refractive index modulation. In each case, as the holes collapse, the value of the refractive index modulation tends towards the same saturation value. In the next section we examine the experimental results and compare those results to the theoretical predictions presented here.

V. EXPERIMENTAL RESULTS

The photopolymer solution is deposited on glass slides and allowed to dry for 48 h. The resulting plates have a thickness of 90 ± 5 μm, which can be measured directly using a micrometer screw gauge. Unslanted transmission holographic gratings were recorded with a spatial frequency of 1000 lines/mm. Recording was carried out using a 532 nm solid-state laser with a recording intensity of 2 mW/cm^2. A 633 nm HeNe laser was used to monitor the first order on-Bragg diffraction efficiency. Short exposure experiments were carried out, each for a different exposure time. Exposure time was controlled using a shutter, which closes after

TABLE IV. Best fit parameters obtained for a 1 s exposure.

Exposure time (s)	$n_{\text{polyacryl}}$	n_{back}	n_{acryl}	τ_n (s)	$\sqrt{\sigma'}$ (nm)	R	D (cm^2/s) ($\times10^{-10}$)	k_H (s^{-1})	ρ	MSE ($\times10^{-11}$)
1	1.511	1.495	1.493	0.09	60	8	2	0.7	0.0005	6.4

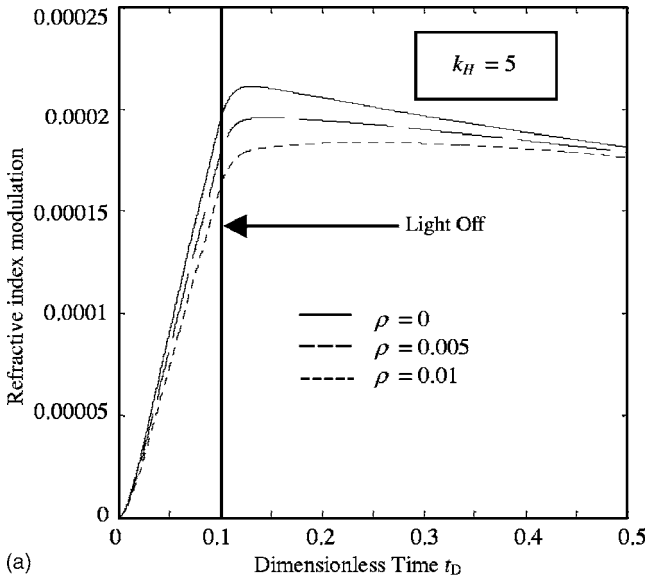

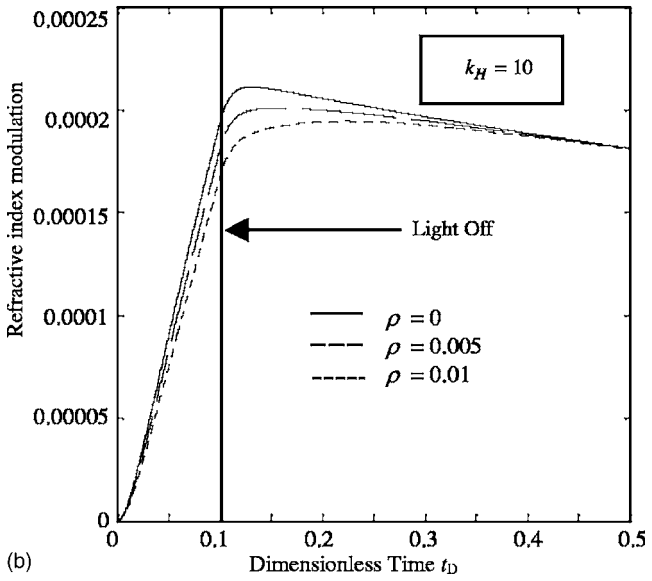

FIG. 3. Theoretical refractive index evolution when (a) k_H=5 and (b) k_H=10 where τ_{nD}=0.01, R_D=1, σ_D=0, α=0, and β=1.

the required recording time has elapsed. We continue to monitor the diffraction efficiency for a period after this point. The results are shown in Fig. 4.

We see a continued slight but rapid increase in diffraction efficiency postexposure followed by a slower decrease before reaching saturation. These results follow closely the form of refractive index evolution predicted by our theoretical simulation described in Secs. III and IV. These simulations are based on the independently determined refractive index measurements of the material components as described in Sec. IV. Therefore the experimental results appear to confirm that the initial growth after exposure is influenced by chain growth and the subsequent slow decrease can be primarily attributed to monomer diffusion.

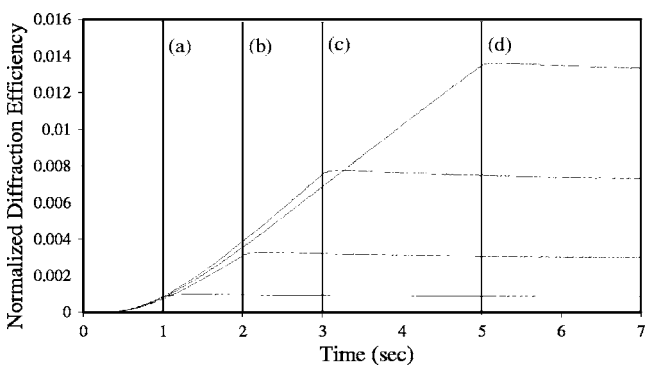

FIG. 4. Diffraction efficiency evolution for short exposures. Exposure times are (a) 1, (b) 2, (c) 3, and (d) 5 s.

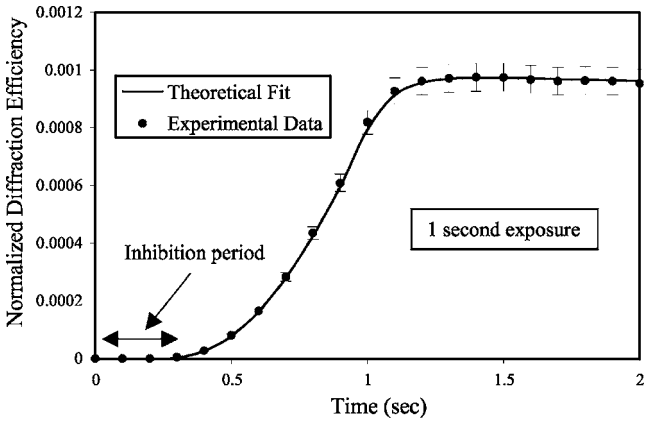

FIG. 5. Fit to experimental data using the best fit parameters given in Table IV for a 1 s exposure.

VI. FITS TO EXPERIMENTAL DATA

In a recent publication fits to this experimental data have been presented for short exposures using the nonlocal model,[24] assuming shrinkage to be negligible. Good fits were achieved with parameter fit values for refractive index corresponding closely to those determined independently.

We now fit the data using the same procedure described in Ref. 24, for the extended model. Examining the experimental data it is evident that the evolution of the profile for each curve is not exactly identical to the previous exposure. However, up to 1 s the repeatability is good. Therefore we apply our fitting procedure to the 1 s exposure data set. The results are shown in Fig. 5.

A good fit is achieved with a mean square error (MSE) of 6.4×10^{-11}. However, the volume of holes relative to the volume of polymer generated over this period is small (ρ=0.005) and the results would appear to support the assumption that for short exposures little or no shrinkage occurs and therefore volume changes do not influence significantly the nature of grating formation examined here. Hole decay, postexposure may also cause some initial grating amplification. However, once again we expect this effect to be small due to the slow hole decay rate and the low concentration of holes generated.

VII. DISCUSSION AND CONCLUSION

In this paper we have investigated the inclusion of a nonlocal temporal response in the NPDD model. The numerical results have shown that as the extent of the nonlocal temporal response changes, the nature of the evolution of the

polymer harmonics at the initial stages of exposure also changes. Examining the effect of the inclusion of this response when modeling grating evolution after exposure has stopped, and based on the assumption that chain termination is not instantaneous, we have carried out numerical simulations, which predict continued polymerization for a period after exposure. We have also extended the nonlocal model to account for material shrinkage, which occurs during the polymerization process, and examined the nature of hole formation and collapse. We have estimated the refractive index of the main components of the photopolymer recording material. Based on these results and the results of the nonlocal diffusion model and using the Lorentz-Lorenz relation we have examined the evolution of the refractive index modulation during short exposures and also immediately postillumination. It has been shown that with the inclusion of a nonlocal temporal response, the index modulation continues to increase after illumination and then decreases as the amplitude of the monomer grating decreases due to monomer diffusion. The initial results would appear to indicate that for short exposure the influence of volume changes in the material is negligible.

We note that this is a first order examination of hole formation in photopolymer and is valid under the assumptions made in Sec. II. The initial results would appear to indicate that it provides a good approximation to the effects of shrinkage on grating formation. However, a more rigorous solution to the NPDD model presented may be necessary to fully describe this behavior. We also note that previously[24] superior fits to experimental data were achieved using the primary termination model ($\beta=2$) when compared to the bimolecular case ($\beta=1$). Further work is necessary to compare these two cases using the model presented here.

ACKNOWLEDGMENTS

The authors acknowledge the support of Enterprise Ireland and Science Foundation Ireland through the through the Research Innovation Fund, the Basic Research Program and the Research Frontiers Program and of the Irish Research Council for Science, Engineering and Technology. One of the authors (J.V.K.) holds an Irish Canadian University Foundation (ICUF) scholarship.

[1] T. D. Milster, Opt. Photonics News **16**, 28 (2005).
[2] L. Dahr *et al.*, *Proceedings of IEEE Conference on Optical Data Storage Conference* (Institute of Electrical and Electronics Engineers, Canada, 2000), pp. 158–160.
[3] *Holographic Data Storage*, Springer Series in Optical Sciences Series, edited by H. J. Coufal, D. Psaltis, and G. T. Sincerbox (Springer, Berlin, 2000).
[4] J. T. Sheridan, M. R. Gleeson, J. V. Kelly, and F. T. O'Neill, Opt. Lett. **30**, 239 (2005).
[5] H. Kobolla, J. T. Sheridan, E. Gluch, J. Schmidt, R. Völkel, J. Schwider, and N. Streibl, J. Mod. Opt. **40**, 613 (1993).
[6] H. Kobolla, J. Schmidt, J. T. Sheridan, N. Streibl, and R. Völkel, J. Mod. Opt. **39**, 881 (1992).
[7] J. Schmidt, R. Völkel, W. Stork, J. T. Sheridan, J. Schwider, N. Streibl, and F. Durst, Opt. Lett. **17**, 1240 (1992).
[8] F. T. O'Neill, A. J. Carr, S. M. Daniels, M. R. Gleeson, J. V. Kelly, J. R. Lawrence, and J. T. Sheridan, J. Mater. Sci. **40**, 4129 (2005).
[9] G. Zhao and P. Mouroulis, J. Mod. Opt. **41**, 1929 (1994).
[10] J. T. Sheridan and J. R. Lawrence, J. Opt. Soc. Am. A **17**, 1108 (2000).
[11] J. H. Kwon, H. C. Chang, and K. C. Woo, J. Opt. Soc. Am. B **16**, 1651 (1999).
[12] G. Odian, *Principles of Polymerization* (Wiley, New York, 1991).
[13] J. R. Lawrence, F. T. O'Neill, and J. T. Sheridan, J. Opt. Soc. Am. B **19**, 621 (2002).
[14] J. R. Lawrence, F. T. O'Neill, and J. T. Sheridan, J. Appl. Phys. **90**, 3142 (2001).
[15] J. V. Kelly, F. T. O'Neill, and J. T. Sheridan, J. Opt. Soc. Am. B **22**, 407 (2005).
[16] S. Blaya, L. Carretero, R. F. Madrigal, M. Ulibarrena, P. Acebal, and A. Fimia, Appl. Phys. B: Lasers Opt. **77**, 639 (2003).
[17] H. M. Karpov, V. V. Obukhovsky, and T. N. Smirnova, Semicond. Phys., Quantum Electron. Optoelectron. **2**, 66 (1999).
[18] R. L. Sutherland, V. P. Tondiglia, L. V. Natarajan, and T. J. Bunning, J. Appl. Phys. **96**, 951 (2004).
[19] S. Wu and E. N. Glytsis, J. Opt. Soc. Am. B **20**, 1177 (2003).
[20] I. Aubrecht, M. Miller, and I. Koudela, J. Mod. Opt. **45**, 1465 (1998).
[21] M. G. Moharam and T. K. Gaylord, J. Opt. Soc. Am. **71**, 811 (1981).
[22] A. V. Galstyan, R. S. Hakobyan, and S. H. T. Galstian, http://www.e-lc.org/Dcuments/T._V_Galstian_2004_05_05_11_13_17.pdf
[23] M. R. Gleeson, J. V. Kelly, C. E. Close, F. T. O'Neill, and J. T. Sheridan, Proc. SPIE **5827**, 232 (2005).
[24] J. V. Kelly, M. R. Gleeson, F. T. O'Neill, J. T. Sheridan, C. Neipp, S. Gallego, and M. Ortuno, Opt. Express **13**, 6990 (2005).
[25] C. Dixon, *Numerical Analysis* (Blackie, Glasgow/London, 1982).
[26] V. L. Colvin, R. G. Larson, A. L. Harris, and M. L. Schilling, J. Appl. Phys. **81**, 5913 (1997).
[27] Metricon Corporation, http://www.metricon.com/appli5.htm#anchor480218
[28] http://chemfinder.cambridgesoft.com
[29] Sigma Aldrich, http://www.sigmaaldrich.com
[30] K. Otmer, *Encyclopedia of Chemical Technology* (Wiley, New York, 1991), Vol. 1.